

Dear Editor,

We would like to thank the reviewers Oliver B. Duffy and Zoe Mildon for their very helpful and insightful comments. Please find attached our revised paper and below a summary of our responses to their comments and suggestions (in red). We have addressed all the reviewers concerns and made the necessary changes.

- 5 In addition to addressing the reviewers comments we have added some additional text and a figure in the discussion section. In the original version we explained that we are considering a limited range of the geometries that can be predicted from this model but did not return to this topic in the discussion. We have included new text in the discussion and an accompanying figure (Fig. 7) that emphasises that the model has the potential to account for a wider range of geometries than those explicitly described in the manuscript. This modification does not change the model or any results but should broaden the  
10 impact and appeal of the manuscript.

If you have any additional questions/comments, please do not hesitate to contact me on stratos.delogkos@ucd.ie.

Yours sincerely,

Efstratios Delogkos, Muhammad Mudasar Saqab, John J. Walsh, Vincent Roche and Conrad Childs.

## 15 **Oliver B. Duffy - Reviewer 1**

1) I suggest the authors add extra sketches (or modify existing sketches in earlier figures) to support section 4.2. as this discussion is relatively complex and difficult to digest.

**Taking into consideration both this and the following comment, this discussion has been modified and references to existing figures have been added. Hopefully this makes it easier to follow.**

- 20 2) In section 4.2. I was finding myself getting a little confused by terminology (e.g. lines 209-210). The use of the term normal drag when referring to ‘monoclines between different stratigraphic sequences or between different fault segments’ needs clarifying. To me, what is described in lines 209-210 and shown in Ferrill et al 2017 (their figure 6) is more reminiscent of a ‘fault-propagation fold’ (e.g. Coleman et al., 2019), but this may be me being confused by the scale or the description. Either way, the terminology can probably be clarified or shown in the sketch as mentioned in Point 1 above.

- 25 **Normal drag, which is defined as the folding adjacent to a fault such that a marker is convex towards the slip direction (see Peacock et al., 2000), is considered to have either a pre-cursory (i.e. fault-propagation fold) or frictional origin. The text has been modified to clarify that in this case the authors refer to the pre-cursory (i.e. fault-propagation fold) origin of normal drag (line 354).**

- 30 3) Perhaps rotate Fig 5b by 90 degrees and put it to the right of 5a so that there is more of a visual link between the two parts.

**Thanks for the suggestion. Figure 5 has been modified accordingly.**

4) Possible references that could be considered for citation:

Spahić, D., Grasemann, B. and Exner, U., 2013. Identifying fault segments from 3D fault drag analysis (Vienna Basin, Austria). *Journal of Structural Geology*, 55, pp.182-195.

35 Long, J.J. and Imber, J., 2010. Geometrically coherent continuous deformation in the volume surrounding a seismically imaged normal fault-array. *Journal of Structural Geology*, 32(2), pp.222-234.

Thanks for bringing these references to our attention.

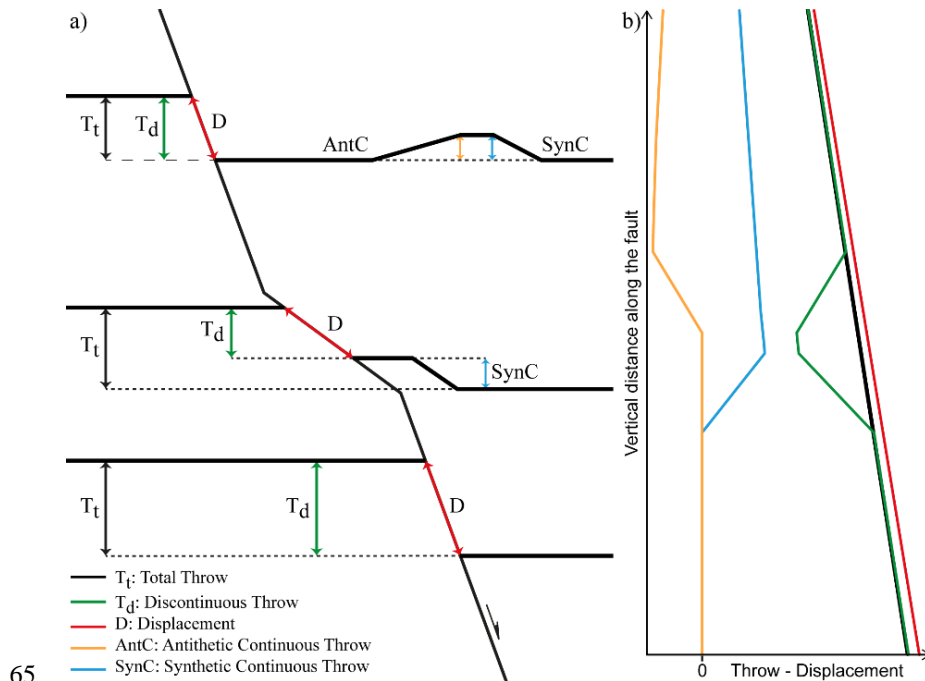
## Zoe Mildon - Reviewer 2

40 1) Initially I was confused reading the manuscript because the authors refer to ‘along-fault bends’, and yet all figures and later discussion refers to concave or convex bends down dip of the fault (contrast this with Faure Walker et al., 2009; Iezzi et al., 2018 who discuss fault bends as changes in strike along the fault scarp at the surface). My interpretation is that the authors are actually discussing “down dip fault bends”, and if this is correct then it should be clarified in the title and abstract of the paper.

45 Yes, the interpretation that we are actually discussing “down-dip fault bends” is correct. Actually, the title of the manuscript refers to “fault-bend folding” and, in literature, as a rule of thumb, “fault-bend folding” refers to the mechanism of folding when the layered rocks fold in response to slip over a down-dip fault bend (Suppe, 1983; Fossen, 2016). However, we understand the cause of confusion and, therefore, we further clarify in the manuscript (including the abstract) that we are discussing about “down-dip fault bends”.

50 2) The assumption of “constant along fault displacement” is clearly stated, but I wonder what the implications of this assumption being incorrect would mean for the conclusions of the paper? For example, Wesnousky, 2008 presents a compilation of historical earthquake ruptures, including normal faulting earthquakes, that show that along a fault the coseismic displacement (and thereby probably the long term displacement) is highly variable. However, there may be confusion on my part given my point in the paragraph above – I think the authors are referring to “constant down-dip fault  
55 displacement” rather than along strike displacement?

It is absolutely correct that fault displacements vary both along strike and down dip with a tendency of the maximum displacement to be located towards the centre of an ideally planar fault surface and its systematic gradual decrease towards the fault tip-lines (e.g. Barnett et al., 1987). In this manuscript, the assumption of “constant along fault displacement” is only a simplification that implicitly excludes displacement variations due to fault propagation related folding and only  
60 concentrates on fault-bend folding. Of course, fault displacement variations are expected (e.g. Walsh et al., 1988) and this doesn’t affect the conclusions for this paper. To illustrate that our deformation algorithm is also valid for the case of variable displacement, the figure below is the equivalent of Figure 2 but, in this case, the displacement systematically decreases upwards with a constant gradient that is not affected by the fault bends. The text has been modified accordingly to clarify this assumption (lines 188-189).



3) Line 37 – “normal faults are often approximately planar” can you provide a reference for this? There are many active normal faults in Italy, Greece and Basin and Range that are not planar (although obviously it depends on the length scale of observation).

70 Yes, faults are rarely planar. However, in this occasion, the authors refer to the normal faults to be approximately planar in comparison to the ramp-flat geometries in thrust systems. The text has been modified accordingly for clarity (lines 142-143).

4) Line 43 – others have investigated strain partitioning and variations in throw along-strike of non-planar normal faults e.g. Faure Walker et al., 2009; Iezzi et al., 2018 – and discussed the implications particularly for seismic hazard.

Thanks for bringing these references to our attention.

75 5) Line 239 – 243 – this is very similar to the conclusion in Iezzi et al., 2018, wherein they looked at the spread of data in the Wells and Coppersmith 1994 data set. Could the observations/models presented in this paper also explain the scatter in fault scaling relationships? Or is this less applicable given the different scale of observation?

Thanks for highlighting this aspect. The presented model can be applied to a wide range of scales, with fault lengths and displacements ranging from a few centimetres up to hundreds of meters (i.e. Figures 5 and 6) and, therefore, we believe that fault throw variations due to down dip fault bend geometries can also provide an explanation in the scatter in fault scaling relationships (e.g. Wells & Coppersmith, 1994). New text has been added to highlight this aspect (lines 396-402).

80 6) Figure 3 – I mostly like this figure, but I am curious about the dots plotted on the graph that refer to the examples presented in the later figures. I’m assuming the dots are plotted according to the dips of the lower and upper fault segment – and then a percentage can be read off the graph. How do these predicted percentages compare to the actual measured

percentages from the seismics/outcrops? This information/analysis seems to be missing from the paper. I think this would be a valuable addition to demonstrate that your simple (but effective!) geometric model works.

The dots in Figure 3 are plotted according to the dips of the lower and upper fault segments to highlight which areas in this plot represent realistic fault-bend geometries. Providing a quantitative comparison between the predicted values and the actual measures, Figure 5b includes the predicted values of the throw components (dashed lines) together with the measured ones (continuous lines).

90

## References

- Barnett, J.A., Mortimer, J., Rippon, J.H., Walsh, J.J. and Watterson, J. Displacement geometry in the volume containing a single normal fault. AAPG Bulletin, 71(8), pp.925-937, 1987.
- Fossen, H.: Structural geology. Cambridge University Press, 2016.
- 95 Peacock, D.C.P., Knipe, R.J. and Sanderson, D.J. Glossary of normal faults. Journal of Structural Geology, 22(3), pp.291-305, 2000.
- Suppe, J.: Geometry and kinematics of fault-bend folding, American Journal of science, 283(7), pp.684-721, 1983.
- Walsh, J.J. and Watterson, J. Analysis of the relationship between displacements and dimensions of faults. Journal of Structural geology, 10(3), pp.239-247, 1988.
- 100 Wells, D.L. and Coppersmith, K.J. New empirical relationships among magnitude, rupture length, rupture width, rupture area, and surface displacement. Bulletin of the seismological Society of America, 84(4), pp.974-1002, 1994.

# Throw variations and strain partitioning associated with fault-bend folding along normal faults

Efstratios Delogkos<sup>1</sup>, Muhammad Mudasar Saqab<sup>1,2</sup>, John J. Walsh<sup>1</sup>, Vincent Roche<sup>1</sup>, Conrad Childs<sup>1</sup>

<sup>1</sup> Fault Analysis Group and iCrag (Irish Centre for Research in Applied Geosciences), UCD School of Earth Sciences, University College Dublin, Belfield, Dublin 4, Ireland

<sup>2</sup> Norwegian Geotechnical Institute, 40 St Georges Terrace, Perth WA 6000, Australia

110 *Correspondence to:* Efstratios Delogkos (stratos.delogkos@ucd.ie, delstratos@hotmail.com)

**Abstract.** Normal faults have irregular geometries on a range of scales arising from different processes including refraction and segmentation. A fault with ~~an average constant~~ dip and ~~constant~~ displacement on a large-scale, will have irregular geometries on smaller scales, the presence of which will generate fault-related folds ~~and , with major implications for~~ ~~across~~ ~~down-fault-throw~~ variations ~~in throw~~. A quantitative model ~~has been~~ presented which illustrates the ~~range of~~ deformation arising from movement on ~~irregular~~ fault surfaces ~~irregularities~~, with fault-bend folding generating geometries reminiscent of normal ~~drag~~ and reverse drag. ~~Calculations based on T~~ the model highlights how ~~along down dip~~ fault ~~displacements~~ ~~throws~~ are partitioned between continuous (i.e. folding) and discontinuous (i.e. discrete ~~displacement~~ ~~offset~~) strain along fault bends ~~characterised by~~ for the full range of ~~possible~~ fault dip changes. ~~These calculations illustrate the~~ ~~potential significance of S~~ strain partitioning on measured fault throw and the potential errors that will arise ~~has a profound~~ ~~effect on measured throw values across faults~~, if account is not taken of the continuous strains accommodated by folding and bed rotations. We show that fault throw can be subject to errors of up to ca. 50% for realistic ~~down-dip~~ fault bend geometries (up to ca. 40°), ~~even~~ on otherwise sub-planar faults with constant displacement. This effect will provide ~~apparently more~~ irregular variations in throw and bed geometries that must be accounted for in associated kinematic interpretations.

## 1 Introduction

125 Fault-bend folding refers to the folding of layered rocks in response to slip over a ~~down-dip fault bend~~ ~~bend in a fault~~ (e.g. Suppe, 1983), an issue which has been the subject of many studies in both extensional (e.g. Deng and McClay, 2019; Groshong, 1989; Williams and Vann, 1987; Xiao and Suppe, 1992) and contractional (e.g. Medwedeff and Suppe, 1997; Suppe, 1983) tectonic settings (Fig. 1). Development of a better understanding of the geometric and kinematic characteristics of fault-bend folding has partly been motivated by several practical challenges, including earthquake hazard assessment (e.g. Chen et al., 2007; Shaw and Suppe, 1996), fault restoration and section balancing (e.g. Gibbs, 1984; Groshong, 1989), hydrocarbon exploration (e.g. Mitra, 1986; Xiao and Suppe, 1989; Withjack et al., 1995) and CO<sub>2</sub> sequestration studies (e.g. Serck and Braathen, 2019).

Previous related work in contractional settings has often focused on understanding and modelling the shapes of folds associated with fault bends (e.g. Boyer and Elliott, 1982; Mitra, 1986; Suppe, 1983; Hardy, 1995; Medwedeff and Suppe,

135 1997; Tavani et al., 2005). This emphasis mainly derives from the importance of fault bends and associated ramp-flat geometries in thrust systems, and from circumstances in which fault-bend folding is often easier to define than the fault displacements that are responsible for its development. Displacement distributions along non-planar thrusts have been examined as an indicator of different fault-bend folding styles (Hughes et al., 2014), but the analysis of displacement variations is much less common than within extensional settings.

140 Normal fault studies have investigated the geometry of hangingwall rollover in relation to the shape (i.e. bends) of listric normal faults (e.g. Gibbs, 1984; Williams and Vann, 1987; Withjack and Schlische, 2006; Xioa and Suppe, 1992; Xiaoli et al., 2015); in particular, but the recognition that normal faults are often approximately planar in comparison to the ramp-flat geometries in thrust systems, has meant that other models are often used to explain the deformation geometries surrounding normal faults, including hangingwall rollover and footwall uplift (e.g. King et al., 1988; Marsden et al., 1990; Roberts and  
145 Yielding, 1994; Healy et al. 2004). Structural studies have therefore often concentrated on defining displacement distributions as a means of investigating fault growth (e.g. Walsh and Watterson, 1988; Scholz et al., 1993; Roche et al., 2012; Torabi et al., 2019), with fewer studies examining the geometries of associated fault-bend folds and the nature of strain partitioning along non-planar normal faults (e.g. Homberg et al., 2017).

In this paper, we present a new quantitative model for the relationship between down-dip fault bend geometry and strain  
150 partitioning along normal faults, and we demonstrate its applicability to different geological examples. We highlight how small-scale irregularities (i.e. bends) are responsible for changes in fault throw, the vertical component of displacement and the pre-eminentmost widely used measure of displacement in the analysis of normal faults. We suggest that a geometrical origin for changes in fault throw is relatively common, since most, if not all, faults have irregular geometries on a range of  
155 linked to the mechanical stratigraphy of the faulted sequence (Wallace, 1861; Peacock and Zhang, 1994; Sibson, 2000; Schöpfer et al., 2007a, b). The local variations in the component of fault throw along fault bends are accommodated by folding (i.e. continuous deformation) and faulting (i.e. discontinuous deformation) and have implications for interpretations of fault growth and for a variety of practical applications, such as (i) across-fault juxtaposition and sealing, (ii) the generation of fault-related traps, both in terms of four-way and three-way dip closures and (iii) assessments of hazard and earthquake  
160 slip.

## 2 Quantitative model of strain partitioning

This study focuses on how strain is locally partitioned at fault bends along normal faults that are approximately planar on large scales. The model assumes that the ~~and have constant~~ vertical component of displacement, referred to here as total throw ( $T_t$ ), is constant and the displacement measured along the fault is also constant (Fig. 2). These circumstances demand  
165 that the discontinuous throw ( $T_d$ ) must change around fault irregularities and the difference between the total throw and the discontinuous throw must be accommodated by deformation of the wall rocks. Wall rock deformation can be in the form of

folding or of minor faults; here we consider only folding as the means of accommodating the difference between  $T_d$  and  $T_c$ . These simple boundary conditions can give rise to a very wide range of behaviours and patterns of wall rock deformation depending on which other assumptions are applied. For illustrative purposes, we present the potential structures developed at  
170 fault bends arising from two additional and relatively conventional assumptions, the implications of which we will discuss later:

(1) Strain of the wall rock is accommodated exclusively by deformation of the hangingwall block with the footwall remaining rigid (i.e. undeformed). ~~This~~ The configuration notion of a relatively undeformed footwall is commonly used and finds support from the relatively subdued nature of footwall, compared to hangingwall, deformation associated with studies  
175 of planar normal faults that intersect the free surface (e.g. King et al., 1988; Roberts and Yielding, 1994; Healy et al., 2004) and is a configuration that is routinely replicated in analogue models.

(2) The hangingwall block is translated parallel to the lower fault segment, with wall-rock deformation accommodating space problems adjacent to the upper fault segment. For example, in the concave extensional case illustrated in Fig. 1 an increase in  $T_d$  on the upper horizon due to the difference in the angle between the upper and lower fault segments  
180 accommodates the space problem caused by the direction of translation of the hangingwall block while the lower horizon remains flat. The option to consider the hangingwall to be translated parallel to the lower fault segment was chosen because this is again routinely replicated in analogue models and the resulting geometries are therefore very familiar (i.e. Fig. 1).

Our deformation algorithm ~~assumes~~ applies a constant along-fault displacement ( $D$ ) and total throw ( $T_c$ ) boundary conditions accommodated by deformation which is neither constant bed length nor constant volume (e.g. Groshong et al., 2012). The  
185 fold geometries are constructed using the method of Groshong (1989) which involves inclined simple shear with axial planes that have a dip equal and opposite to that of the fault surface (Figs 1, 2 and 4): other methods could have been applied but the principal conclusions relating to variations in partitioning of discontinuous and continuous throws would have been similar. The basic findings of our modelling are also applicable to faults with gradually changing displacements in line with established displacement-length scaling and displacement gradients on faults (e.g. Nicol et al., 2020). Constant along-fault  
190 displacement implicitly assumes no propagation-related folding (i.e. Coleman et al., 2019) or associated displacement changes, a reasonable simplifying condition for our study concentrating on fault-bend folding. ~~Figure~~ Fig. 2 shows that in these circumstances strain will be accommodated by discontinuous (e.g. fault-related) and continuous (e.g. fold-related) deformation adjacent to fault bends, the nature of which is described below. ~~For illustration purposes, the shape of the folds (i.e. the hangingwall deformation) is designed by assuming inclined simple shear with axial planes that have a dip equal and~~  
195 ~~opposite to that of the fault surface (Figs 1, 2 and 4; Groshong, 1989).~~

Constant ~~along~~ fault displacement ( $D$ ) ~~means~~ requires, for example, that the ~~along fault~~ discontinuous throw ( $T_d$ ) decreases ~~along fault~~ above a bends ~~that where a fault~~ steepens downwards and is compensated by an increase in continuous throw ( $T_c$ ;  
Fig. 2) accommodating deformation of the wall rock in the form of folding. In that sense the development of folding ~~along~~ above  
200 above a fault bend is complementary to the discontinuous throw and contributes to the conservation of a constant total throw across the fault ( $T_c$ ; Fig. 2). For this case of a fault ~~bend~~ which steepens downwards, and is ~~therefore~~ convex to the

205 hangingwall, (i.e. Fig. 1) the continuous component of throw is referred to as synthetic continuous throw ( $S_{yn}C$ ) insofar as it complements and aggregates with the discontinuous throw ( $T_d$ ) to provide the constant total throw (i.e.  $T_t = T_d + S_{yn}C$ ). By contrast, for a fault bend which shallows downwards, and is concave towards the hangingwall (i.e. Fig. 1), the continuous throw is referred to as antithetic continuous throw ( $A_{nt}C$ ) with the total throw equivalent to the difference between the discontinuous and continuous components of throw (i.e.  $T_t = T_d - A_{nt}C$ ). Synthetic and antithetic continuous throws accommodate down to the hangingwall and footwall bed rotations, respectively, and in that sense are reminiscent of normal ~~drag~~ and reverse drag bed deformations (Barnett et al. 1987), even if their origin is very different (see below). ~~Using this simple model, we investigate below the basic deformation geometries associated with local fault bends along a selection of normal faults.~~

210 The relative magnitudes of  $T_d$  and  $T_t$  for the simplest case of a sharp fault bend comprising only two fault segments and horizontal pre-faulting bedding (i.e. Fig. 1), is given by

~~the simplest case of a sharp fault bend comprising only two fault segments (i.e. Fig. 1), partitioning of the total throw onto the discontinuous and continuous throws can be calculated for a horizon with both footwall and hangingwall fault cutoffs along the upper fault segment (i.e. the grey layer in Fig. 1), as follows:~~

215 
$$\frac{T_d}{T_t} = \frac{\sin\beta}{\sin\alpha} \quad (1), \text{ and } \frac{T_c}{T_t} = 1 - \frac{T_d}{T_t} \quad (2),$$

where  ~~$T_d$  is the discontinuous throw,  $T_c$  is the continuous throw,  $T_t$  is the total throw, and  $\alpha$  and  $\beta$  are the dips of the lower and upper fault segments, respectively (Fig. 1). Figure Fig. 3(a) illustrates the outcome of these calculations (Eq. 1 and 2 expressed as a percentage)~~ for the whole range of fault dips while Fig. 3(b) shows the complementary values for the continuous throw ( $T_c$ ). ~~As expected,~~ In the absence of a bend (i.e. where the lower and upper fault segments have the same

220 dip) the entire total throw is discontinuous. Fault bends which are concave towards the hangingwall show a local increase in discontinuous fault throw on layers with cutoffs straddling the fault bend, whereas faults bends which are convex to the hangingwall show a local decrease in discontinuous throw. The discontinuous throw is therefore less than the total throw for convex fault bends and larger for concave fault bends (Fig. 3). For example, a convex fault bend with a  $70^\circ$  dip of the lower fault segment and a  $45^\circ$  dip of the upper fault segment will accommodate ca. 75 percent of the total throw by discontinuous  
225 throw and the remaining ca. 25 percent by continuous throw (Fig. 3). The negative values of continuous throw for concave fault bends at Fig. 3b represent the antithetic continuous throw that, as mentioned above, contributes negatively to the total throw.

As the throw on a fault surface increases the significance of the throw partitioning due to a bend will decrease. The plots in Fig. 3 are appropriate to the situation in which the hangingwall cut-off of an offset horizon lies above the bend in the fault  
230 (time 1 in Fig. 4). While this condition is maintained, Based on Eqs 1 and 2, a progressive an increase in fault displacement results in a progressive increase of the absolute amount of in continuous deformation while so that its proportion to of the total throw remains constant (from time 1 to time 2 in Fig. 4). However, as soon as once the hangingwall fault cutoff reaches the bend and begins to move along the lower fault segment (from time 2 to time 3 in Fig. 4), the absolute amount of

continuous deformation ~~doesn't increase anymore further remains constant resulting and becomes in~~ a progressively smaller  
235 ~~proportion of the total throw, decrease of its proportion to the total throw as the displacement increases.~~

Faults however often extend beyond a single bend, as illustrated for the fault in Fig. 2a which comprises three fault  
segments forming two sharp bends, a lower convex and an upper concave bend. In this case, synthetic continuous  
deformation is developed along the middle and upper fault segments as a result of the lower convex bend. By contrast,  
antithetic continuous deformation is developed only along the upper segment as a result of the upper concave bend. The  
240 partitioning of displacement across fault bends therefore varies spatially with an individual bed showing multiple  
deformations depending on how many bends an individual bed is offset across. The main principles of how the strain is  
partitioned along these fault bends are highlighted by the throw-displacement profiles in Fig. 2b, with complementary  
variations of the discontinuous and continuous (both, synthetic and antithetic) throws resulting in our prescribed constant  
total throw ( $T$ ), given that the displacement ( $D$ ) is also constant.

245 Whilst our treatment is relatively simple insofar as fault bends in nature are rarely single sharp bends, our comparison with  
natural examples below shows that the basic conclusions drawn from our analysis can be applied to more continuously  
curved bends which are perhaps best considered as continuously curved multiple bend faults (e.g. Medwedeff and Suppe,  
1997; Shaw et al., 2005; Withjack et al., 1995). This is because the commonly observed continuously curved fault bends (i.e.  
Figs 5 and 6) can be treated as multiple sharp fault bends consisting of many small, planar, fault segments (e.g. Xiao and  
250 Suppe, 1992).

### 3 Geological examples

A selection of natural faults displaying fault bends and associated folding is presented from seismic (Figs 5 and 6a) and  
outcrop (Figs 6b and 6c) datasets. These examples highlight the principal features of relatively simple normal faults  
displaying similar characteristics to those illustrated in Figs 1, 2 and 4, demonstrating the applicability of the proposed  
255 quantitative model of strain partitioning. Some of the fault bend geometries present along the following natural faults are  
plotted in Fig. 3 to provide an appreciation of which areas at these plots (Fig. 3) represent realistic fault bend geometries.

#### 3.1 Porcupine Basin, offshore Ireland

A normal fault imaged on, depth-converted seismic reflection data from the northwestern Porcupine Basin, offshore west  
Ireland (Fig. 5; Worthington and Walsh, 2017), has a maximum total throw of ca. 600 m accommodated along a  
260 continuously curved fault surface with a sigmoidal shape, and comprising both convex and concave bends (Fig. 5a).  
Accumulation of displacement has resulted in deformation of the hangingwall in the form of anticlinal and monoclinical  
structures associated with these bends. The throw-displacement profiles along this normal fault indicate that the  
discontinuous and continuous throws are complementary to each other so that the distribution of their sum (i.e. the total  
throw) is not affected by the fault bend (Fig. 5b). The distribution of the displacement is not affected by the fault bend

265 suggesting the validity of the assumptions of the proposed model, with modelled discontinuous and continuous throws showing a good fit to the measured throws (Fig. 5b).

An interesting feature of this fault is that the hangingwall rollover geometry associated with the upper part of the fault surface appears to be accommodated by smaller-scale antithetic faults which are close to the limit of seismic resolution. This is a characteristic of all apparently ductile and continuous deformation, insofar as it can be accommodated by smaller-scale faulting (i.e. brittle deformation), with, for example, reverse drag and normal drag accommodated by antithetic and synthetic faulting, respectively (Hamblin, 1965; Walsh & Watterson, 1991; Walsh et al., 1996).

### 3.2 Taranaki Basin, offshore New Zealand

A normal fault imaged on high quality, depth converted, seismic reflection data from the northern Taranaki Basin, offshore west New Zealand (Fig. 6a; Giba et al., 2012). It has a maximum total throw of ca. 900 m which is again accommodated along a continuously curved fault surface with a sigmoidal shape which comprises both convex and concave bends (Fig. 6a). In this case, fault displacement relative to fault bend geometry generates the full range of folding, with antithetic and synthetic shear associated with shallowing and steepening bends respectively. Due to the decrease in along-fault discontinuous throw associated with the shallower parts of the fault surface, preservation of the total throw is accommodated by a concomitant increase in synthetic shear as the fault steepens at greater depths (i.e. pink horizon at Fig. 6a). Conversely, due to the upper concave bend, antithetic shear is generated which is partly accommodated by minor antithetic faults and results in the formation of an anticlinal rollover structure. These deformations indicate that the discontinuous throws along a fault surface do not account for the total throw which should, instead, take account of the fault-related folding, with, for example, the aggregation of discontinuous fault throw and synthetic/antithetic shears.

The origin of fault bending for this example, illustrates that fault bends need not be simple cylindrical sub-horizontal bends arising from fault refraction through different mechanical layers. The observed fault bend arises from twisting and segmentation of an upward propagating fault, circumstances that have generated a left-hand bend arising from left stepping in map view into the plane of observation (see Giba et al., 2012 for further details). This configuration generates both lateral and vertical changes in the discontinuous throw which are not representative of the throw across the fault unless account is taken of the associated fault-bend folding.

### 290 3.3 Wadi Matulla, Sinai, Egypt

A normal fault within the Coniacian-Santonian Matulla Formation which contains mixed siliciclastic and carbonate sediments (Fig. 6b; Fossen, 2016; Sharib et al., 2019). The fault with an estimated throw of ca. 3 m shows a rollover anticline associated with a fault surface which has a sigmoidal shape comprising both convex and concave bends (Fig. 6b). This outcrop example clearly illustrates that a significant proportion of the deformation associated with fault-bend folding (i.e. anticline) can be accommodated by minor antithetic and/or synthetic faulting.

### 3.4 Kilve, Somerset, UK

Upper Jurassic normal faults within the Liassic limestone-shale sequences of Kilve often show near-fault deformations associated with fault surface irregularities arising from fault refraction (Peacock and Zhang, 1994; Schöpfer et al., 2007a, b), in which faults are steeper within limestones and shallower within shales. The significance of associated fault-bend folds varies with the nature of the host-rock stratigraphy and with fault displacement, with smaller folds transected by more through-going fault surfaces at higher displacements (Schöpfer et al., 2007a, b). Fig. 6c shows a fault with hangingwall normal drag associated with a downward steepening fault generated by a triplet of limestone beds bounded by overlying and underlying shales. Displacement is on the same scale as the triplet of layers and fault-related folding is already bounded and/or bypassed by what are interpreted to be newly developed slip surfaces.

## 305 4 Discussion

### 4.1 Model assumptions

The proposed quantitative model of strain partitioning along non-planar faults assumes that the displacement and the total throw are constant, as illustrated in Fig. 2, or vary systematically in line with the D-L scaling and the displacement gradients observed on faults (e.g. Nicol et al., 2020). A consequence of this assumption is that the bed length and/or thickness may not remain constant during deformation. This is in contrast with the fault-bend folding theory proposed by Suppe (1983) that assumes conservation of area and constant layer thickness implying conservation of bed length and abrupt changes of the displacement at fault bends. While this theory has been extensively applied to compressional settings, it may not be valid ~~to~~ for extensional settings given that it is geometrically impossible to preserve the layer thickness along non-planar faults that have steep fault dips relative to bedding (Suppe, 1983). This is consistent with other studies suggesting that bed length and/or thickness does not remain constant during: (i) displacement accumulation along fault bends in both, compressional (e.g. Groshong et al., 2012) and extensional (Poblet and Bulnes, 2005; Xiao and Suppe, 1992) settings, (ii) the accommodation of displacement gradients along planar faults (e.g. Barnett et al., 1987) and (iii) the strains associated with vertically segmented faults (e.g. Childs et al., 1996). Taken together the available evidence supports the notion that bed length and/or thickness changes can accommodate the strains and folding associated with either constant or slowly changing displacement and total throw along non-planar faults. Typical deformations adjacent to normal faults include normal drag or reverse drag folding, sometimes accommodated by minor faults.

The hangingwall deformation associated with fault bends is generally considered to be accommodated only by continuous deformation i.e. folding and ductile strain. However, examples of fault bends in outcrops (e.g. Fig. 6b), experimental models (e.g. Withjack and Schlische, 2006) and high-resolution seismic reflection data (e.g. Fig. 6a) indicate that a proportion of the hangingwall deformation can be accommodated by secondary faulting, that is synthetic and/or antithetic to the main fault (e.g. Fig. 6). Whether hangingwall deformation is accommodated by folding and/or secondary faulting will depend on the

mechanical properties of the faulted sequence and ~~the amount and the strain~~ rate of shear strain accommodated. Differentiation between these two deformation components will largely depend on the quality and resolution of the available data: for example, seismic datasets will image hangingwall deformation as a ductile strain when it is accommodated by faults with displacements below seismic resolution (up to 20m throw for good quality seismic; Walsh et al., 1996).

The basic assumption of the model, that displacement and total throw are constant, or vary in a regular manner down a fault trace, provides a basis for evaluating the partitioning of the total throw into discontinuous throw at the fault surface and continuous throw accommodated by wall rock deformation. These conditions can be fulfilled in many ways and by a range of different deformation geometries. This paper considers a small subset of these geometries as it is restricted to the case where only the hangingwall is deformed and translation of the hangingwall is parallel to the fault trace below the fault bend (i.e. Fig. 1). These restrictions allow for calculation of unique values for throw partitioning for any combination of fault dips above and below a bend (Fig. 3). This restricted case was addressed because it generates geometries that are familiar from seismic mapping and from analogue models of deformation of a cover sequence above a rigid basement. However, for bends on blind faults or parts of faults that are distant from the free surface, there is no reason to expect that either of these restrictions applies and it is possible that fault bends will impact equally on the footwall and hangingwall and on horizons above and below a bend. The range of wall rock geometries that could be predicted from this model is therefore much broader than using our more restricted case: this broader range could even provide end-member geometries at bends on blind faults that, for example, are the equivalent of viewing Fig. 1 upside down. Many of these, and other geometries that can be considered, appear unlikely and may not occur in nature but many do. For example, Fig. 7 shows a field sketch in which local reverse drag in the footwall of a fault with a maximum throw of ca. 20 cm appears to occur in response to an upward shallowing of the fault in a geometry that is the upside down equivalent of a hangingwall rollover (inset Fig. 7). Whilst these considerations suggest that there may be a range of near-fault horizon geometries due to fault surface irregularities, our approach allows us to investigate the variations in throw and strain partitioning along faults with bends, rather than to define the precise nature of the deformation along a particular fault.

## 4.2 Evolution of fault zones

Any fault characterized by fault bends will show associated folding and/or bed rotations of the host rock. These deformations will be reminiscent of both normal and reverse drag folding which are, respectively, in sympathy with, or in opposition to, the sense of shear accommodated by the fault. Normal drag is often considered to be pre-cursory (i.e. fault-propagation fold; Fig. 1 in Coleman et al., 2019), forming as monoclines between different stratigraphic sequences (i.e. Ferrill et al., 2017) or between different fault segments (i.e. Childs et al., 2017). Normal fault surfaces which are convex towards the hangingwall, and downward steepening, will however generate hangingwall normal drag (e.g. convex fault bend in Fig. 4), a phenomenon which accompanies fault movement and is geometrically and mechanically equivalent to so-called frictional drag (i.e. Peacock et al., 2000; Davis et al., 2011; Fig. 1 in Coleman et al., 2019) but on a macroscopic rather than microscopic scale. Reverse drag is generally attributed to ~~much larger~~ scale bed rotations that are in opposition to the fault-parallel shear, giving

360 rise to hangingwall rollover and footwall uplift associated with normal faults, whether they have listric or planar geometries (Barnett et al., 1987). Since conventional reverse drag occurs on much greater length scales than those considered here (i.e. approaching the length of a fault rather than that of a fault bend), any geometrical similarity, and localized steepening of bed dips in opposition to fault dip (e.g. concave fault bend in Fig. 4), is linked to fault bend geometry (and downward shallowing) rather than conventional reverse drag. Whatever the nature of drag, with subsequent growth these deformed host  
365 rocks will often be bypassed by through-going slip surfaces, to provide a fault zone with rotated packages of host rock bounded by slip surfaces. For displacements which are larger than the scale of fault bends, host rock deformation will be cumulative and whilst it is, in principle, possible that beds could become more folded, increased fault displacement is more likely to provide increasing cumulative deformation leading to progressive fault rock generation. In that sense, the presence of fault bends will provide the locus of fault rock generation as displacements accumulate with fault growth, a model that is  
370 aligned with the geometric model for fault zone growth outlined by Childs et al., 2009.

### 4.3 Implications

Since fault throw is the most commonly used measure of fault offset in extensional fault systems, an important implication of the proposed model is that the throw measured at normal fault surfaces varies with fault bends and irregularities. On an approximately planar fault surface with constant total throw, relatively smaller scale bends can lead to local discontinuous  
375 fault throws which are greater or less than the total throw. Previous work shows that whilst-while fault throws vary systematically along the length of individual faults, smaller scale variations can occur (e.g. Walsh and Watterson, 1987; Cartwright and Mansfield, 1998; Manighetti et al., 2001; Nixon et al., 2014; Childs et al., 2017). Our quantitative model suggests that some of those variations arise from local changes in fault geometry such as those accompanying the generation of fault segments and fault refraction processes that can occur on a range of scales even on the same fault. These local effects  
380 are best accounted for by either including near-field bed rotations or by measuring fault throws from hangingwall and footwall bed elevations beyond the near-near-field bend-related deformations adjacent to fault surfaces. Accounting for this partitioning of throw will lead to along-fault throw variations which are more systematic than local throw values, suggesting a scenario which reflects the coherence of throw changes on faults with associated propagation-related complexities, such as refraction and segmentation. Whatever the nature and origin of fault bends, our quantitative model suggests that throw  
385 measurements that do not incorporate bend-related deformations will-may be subject to throw errors of up to ca. 50% for realistic fault bend geometries; which are nevertheless towards the upper end of what is likely in nature (up to ca. 40°; Figs 3, 5 and 6). However, even for modest fault bends of up to 10°, on faults with characteristic normal fault dips larger than ca. 50°, apparent throw variations of ca. 10% are predicted.

The presence of fault bends and associated deformation can also have implications for a variety of practical purposes. The  
390 partitioning of fault displacement into continuous rather than discontinuous deformation will affect across-fault juxtapositions, and if developed at sub-seismic scales can have a profound impact on fault seal assessments. The development of associated folding can also generate potential fault -controlled-bend-related hangingwall traps, both in terms

of three- and four-way dip closures, to either hydrocarbons or mineral systems. Furthermore, the deformation of the host rock sequence due to the down-dip fault surface irregularities should be considered when assessing hazards and earthquake slips because fault scarp dips can be ill-defined dip-wise, with easily measured discontinuous throw varying with fault bend geometries. Previous studies on coseismic throw variations along surface ruptures (e.g. Faure Walker et al., 2009; Jazzi et al., 2018) have also identified strain partitioning associated with fault dip changes in along-strike bends that were attributed to both lateral and up-dip propagation of two faults that are non-colinear. Our model is consistent with those observations and can also be reconciled with other kinematic interpretations, such as the exclusively up-dip propagation, bifurcation and twisting of a single fault. Whatever their precise kinematic origin, these fault throw variations, as Jazzi et al. 2018 have demonstrated, can also explain the scatter in maximum offset versus surface rupture length scaling relationships (e.g. Wells & Coppersmith, 1994).

## 5 Conclusions

- (i) A quantitative model has been presented for the throw variations and strain partitioning associated with fault-bend folding along normal faults with fault surface irregularities arising from propagation-related phenomenon (e.g. refraction or segmentation).
- (ii) The main feature of this model is that the variations of discontinuous and continuous throws along non-planar normal faults are complementary given that the displacement and total throw are constant and not affected by the fault bends.
- (iii) This model shows that small-scale normal and reverse drag arise from fault bends that steepen or shallow downwards, respectively. Normal drag in this case arises from deformation which is equivalent to macroscopic scale frictional drag rather than a pre-cursory phenomenon.
- (iv) Whatever the nature of fault-bend folding, it can have a significant effect on the measured across-fault throw, the main measure used for quantifying fault displacements on offset across normal faults.
- (v) The fault throw can be subject to errors of up to ca. 10% and ca. 50% for fault bend geometries of between ca. 10° and 40° respectively, even on otherwise sub-planar faults with constant displacement.
- (vi) Fault-bend folding will be developed in mechanically anisotropic host rock sequences where processes such as refraction and segmentation are promoted, and failure to identify their significance will lead to erroneous kinematic interpretations.
- (vii) Fault-bend folding is expected to occur on a range of scales that are related to the mechanical stratigraphy.

## Acknowledgements

This publication has emanated from research supported in part by a research grant from Science Foundation Ireland (SFI) under Grant Number 13/RC/2092 and co-funded under the European Regional Development Fund and by PIPCO RSG and its member companies. We gratefully acknowledge the Petroleum Affairs Division (PAD) of the Department of

Communications, Climate Action and Environment (DCCAE), Ireland, for providing the seismic and well data. The authors would like to thank Schlumberger for providing access to Petrel software. Thanks also to other members of the Fault Analysis Group for useful technical discussions. We also thank Oliver B. Duffy and Zoe Mildon for their helpful reviews, and Mark Allen for editorial handling.

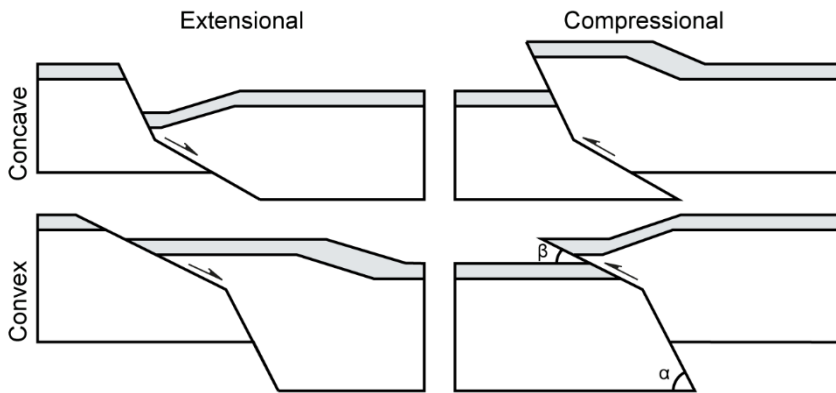
## References

- Barnett, J.A., Mortimer, J., Rippon, J.H., Walsh, J.J., and Watterson, J.: Displacement geometry in the volume containing a single normal fault, AAPG Bulletin, 71(8), pp.925-937, 1987.
- 430 Boyer, S.E., and Elliott, D.: Thrust systems, AAPG Bulletin, 66, 1196-1230, 1982.
- Cartwright, J.A., and Mansfield, C.S.: Lateral displacement variation and lateral tip geometry of normal faults in the Canyonlands National Park, Utah, Journal of Structural Geology, 20(1), pp.3-19, 1998.
- Chen, Y.G., Lai, K.Y., Lee, Y.H., Suppe, J., Chen, W.S., Lin, Y.N.N., Wang, Y., Hung, J.H., and Kuo, Y.T.: Coseismic fold scarps and their kinematic behavior in the 1999 Chi-Chi earthquake Taiwan, Journal of Geophysical Research: Solid Earth, 435 112(B3), 2007.
- Childs, C., Nicol, A., Walsh, J.J., and Watterson, J.: Growth of vertically segmented normal faults, Journal of Structural Geology, 18(12), pp.1389-1397, 1996.
- Childs, C., Manzocchi, T., Walsh, J.J., Bonson, C.G., Nicol, A., and Schöpfer, M.P.J.: A geometric model of fault zone and fault rock thickness variations, Journal of Structural Geology, 31, 117-127, 2009.
- 440 Childs, C., Manzocchi, T., Nicol, A., Walsh, J.J., Soden, A.M., Conneally, J.C., and Delogkos, E.: The relationship between normal drag, relay ramp aspect ratio and fault zone structure, Geological Society, London, Special Publications, 439(1), pp.355-372, 2017.
- Coleman, J.A., Duffy, B.O., Jackson, A-L.C.: Growth folds above propagating normal faults, Earth-Science Reviews, 126, 102885, 2019.
- 445 [Davis, G.H., Reynolds, S.J. and Kluth, C.F. Structural geology of rocks and regions. John Wiley & Sons, 2011.](#)
- Deng, H., and McClay, K.: Development of extensional fault and fold system: Insights from 3D seismic interpretation of the Enderby Terrace, NW Shelf of Australia, Marine and Petroleum Geology, 104, pp.11-28, 2019.
- Ferrill, D.A., Morris, A.P., McGinnis, R.N., and Smart, K.J.: Myths about normal faulting, Geological Society, London, Special Publications 439 (1), 41-56, 2017.
- 450 Fossen, H.: Structural geology. Cambridge University Press, 2016.
- Giba, M., Walsh, J.J., and Nicol, A.: Segmentation and growth of an obliquely reactivated normal fault, Journal of Structural Geology, 39, pp.253-267, 2012.
- Gibbs, A.D.: Structural evolution of extensional basin margins, Journal of the Geological Society, 141(4), pp.609-620, 1984.

- Groshong Jr, R.H.: Half-graben structures: Balanced models of extensional fault-bend folds, Geological Society of America Bulletin, 101(1), pp.96-105, 1989.
- Groshong Jr, R.H., Withjack, M.O., Schlische, R.W., and Hidayah, T.N.: Bed length does not remain constant during deformation: Recognition and why it matters, Journal of Structural Geology, 41, pp.86-97, 2012.
- Hamblin, W.K.: Origin of "Revere drag" on the downthrown side of normal faults, GSA Bull., 76(10), pp.1145-1164, 1965.
- Hardy, S.: A method for quantifying the kinematics of fault-bend folding, J. Struct. Geol., 17(12), 1785-1788, 1995.
- 460 Healy, D., Yielding, G., and Kusznir, N.: Fracture prediction for the 1980 El Asnam, Algeria earthquake via elastic dislocation modeling, Tectonics, 23, TC6005, 2004.
- Homberg, C., Schnyder, J., Roche, V., Leonardi, V., and Benzaggagh, M.: The brittle and ductile components of displacement along fault zones. Geological Society, London, Special Publications, 439(1), pp.395-412, 2017.
- Hughes, A.N., and Shaw, J.H.: Fault displacement-distance relationships as indicators of contractional fault-related folding style, AAPG bulletin, 98(2), pp.227-251, 2014.
- 465 [Iezzi, F., Mildon, Z., Walker, J.F., Roberts, G., Goodall, H., Wilkinson, M. and Robertson, J. Coseismic throw variation across along-strike bends on active normal faults: Implications for displacement versus length scaling of earthquake ruptures. Journal of Geophysical Research: Solid Earth, 123\(11\), pp.9817-9841, 2018.](#)
- King, G.C.P., Stein, R.S., and Rundle, J.B.: The growth of geological structures by repeated earthquakes 1. Conceptual framework, Journal of Geophysical Research: Solid Earth 93 (B11), 13307-13318, 1988.
- 470 Manighetti, I., King, G.C.P., Gaudemer, Y., Scholz, C.H., and Doubre, C.: Slip accumulation and lateral propagation of active normal faults in Afar, Journal of Geophysical Research: Solid Earth, 106(B7), pp.13667-13696, 2001.
- Marsden, G., Yielding, G., Roberts, A.M., and Kusznir, N.J.: Application of a flexural cantilever simple-shear/pure shear model of continental lithosphere extension to the formation of the northern North Sea basin. In: Tectonic evolution of the North Sea rifts, Oxford McClay, K.R.: Extensional fault systems in sedimentary basins: a review of analogue model studies. Marine and petroleum Geology, 7(3), pp.206-233 University Press Oxford, pp. 241-261, 1990.
- 475 Medwedeff, D.A., and Suppe, J.: Multibend fault-bend folding, Journal of Structural Geology, 19(3-4), pp.279-292, 1997.
- Mitra, S.: Duplex structures and imbricate thrust systems: Geometry, structural position, and hydrocarbon potential, AAPG Bulletin, 70, 1087-1112, 1986.
- 480 Nicol, A., Walsh, J.J., Childs, C., and Manzocchi, T.: The growth of faults. In: Understanding Faults: Detecting, Dating, and Modeling. (Edited by Tanner, D., and Brandes, C.). Elsevier, ISBN: 9780128159859, 2020.
- Nixon, C.W., Sanderson, D.J., Dee, S.J., Bull, J.M., Humphreys, R.J., and Swanson, M.H.: Fault interactions and reactivation within a normal-fault network at Milne Point, Alaska, AAPG Bulletin, 98(10), pp.2081-2107, 2014.
- Peacock, D.C.P., and Zhang, X.: Field examples and numerical modelling of oversteps and bends along normal faults in cross-section, Tectonophysics, 234 (1-2), 147-167, 1994.
- 485 [Peacock, D.C.P., Knipe, R.J., and Sanderson, D.J.: Glossary of normal faults, Journal of Structural Geology, 22\(3\), pp.291-305, 2000.](#)

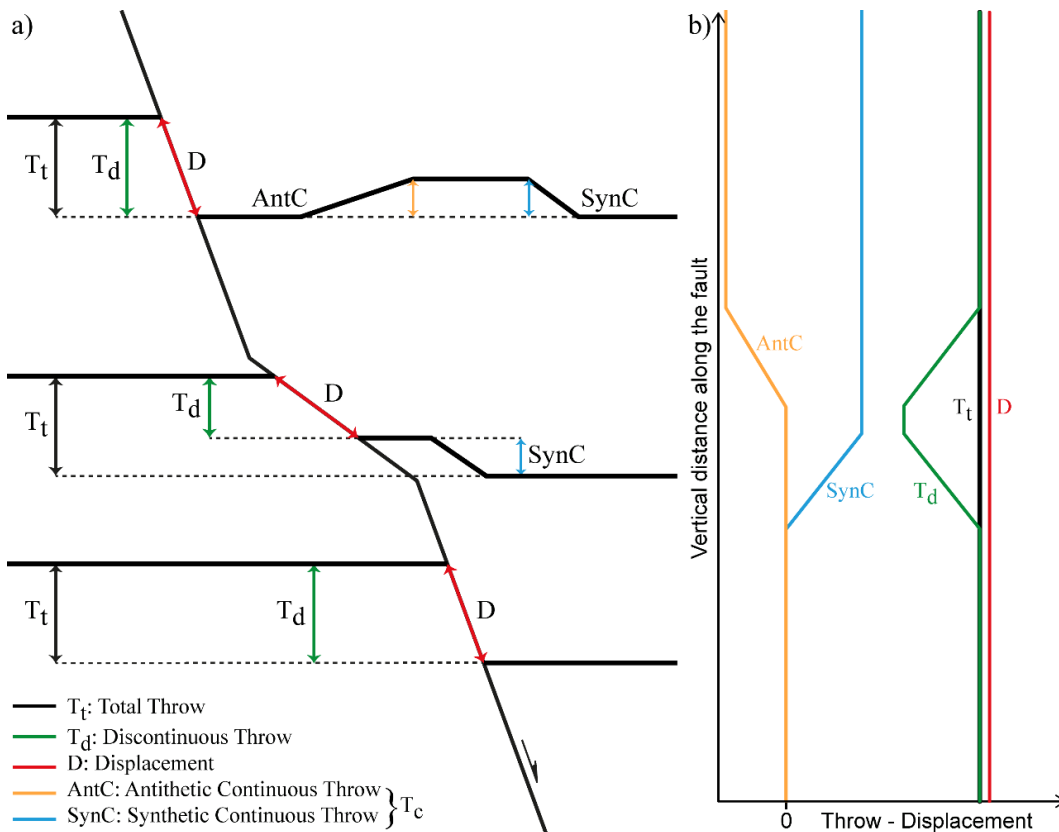
- Poblet, J., and Bulnes, M.: Fault-slip, bed-length and area variations in experimental rollover anticlines over listric normal faults: influence in extension and depth to detachment estimations, *Tectonophysics*, 396(1-2), pp.97-117, 2005.
- 490 Roberts, A., and Yielding, G.: Continental extensional tectonics. In: *Continental Deformation*. Pergamon Press, Oxford, 223-250, 1994.
- Roche, V., Homberg, C., and Rocher, M.: Fault displacement profiles in multilayer systems: from fault restriction to fault propagation, *Terra Nova*, 24(6), pp.499-504, 2012.
- Serck, S.C., and Braathen A.: Extensional fault and fold growth: impact on accommodation evolution and sedimentary infill, 495 *Basin Research*, 31(5), pp.967-990, 2019.
- Schöpfer, M.P.J., Childs, C., and Walsh, J.J.: 2D Distinct Element modeling of the structure and growth of normal faults in multilayer sequences. Part 1: Model calibration, boundary conditions and selected results, *Journal of Geophysical Research* 112, B10401, 2007a.
- Schöpfer, M.P.J., Childs, C., Walsh, J.J., Manzocchi, T., and Koyi, H.A.: Geometrical analysis of the refraction and 500 segmentation of normal faults in periodically layered sequences, *Journal of Structural Geology*, 29, pp. 318-335, 2007b.
- Sharib, A., Ahmed, S.A.A., Selim, A.Q., Abdel Fattah, M.M., Hassan, S.M., and Sanislav, I.V.: Thermal Alteration of Organic Matter in the Contact of a Rift-Related Basaltic Dyke: An Example from the Black Limestone, Wadi Matulla, West Central Sinai, Egypt, *Minerals*, 9(5), p.279, 2019.
- Shaw, J.H., Connors, C.D., and Suppe, J. eds.: *Seismic interpretation of contractional fault-related folds: An AAPG seismic atlas* (Vol. 53), AAPG, 2005.
- 505 Shaw, J.H., and Suppe, J.: Earthquake hazards of active blind-thrust faults under the central Los Angeles basin, California, *Journal of Geophysical Research: Solid Earth*, 101(B4), pp.8623-8642, 1996.
- Scholz, C.H., Dawers, N.H., Yu, J.Z., Anders, M.H., and Cowie, P.A.: Fault growth and fault scaling laws: preliminary results, *Journal of Geophysical Research: Solid Earth*, 98(B12), pp.21951-21961, 1993.
- 510 Sibson, R.H.: Fluid involvement in normal faulting, *Journal of Geodynamics*, 29(3-5), pp.469-499, 2000.
- Suppe, J.: Geometry and kinematics of fault-bend folding, *American Journal of science*, 283(7), pp.684-721, 1983.
- Tavani, S., Storti, F., and Salvini, F.: Rounding hinges to fault-bend folding: geometric and kinematic implications, *Journal of Structural Geology*, 27(1), pp.3-22, 2005.
- Torabi, A., Alaei, B. and Libak, A.: Normal fault 3D geometry and displacement revisited: Insights from faults in the 515 Norwegian Barents Sea, *Marine and Petroleum Geology*, 99, pp.135-155, 2019.
- [Walker, J.F., Roberts, G.P., Cowie, P.A., Papanikolaou, I.D., Sammonds, P.R., Michetti, A.M. and Phillips, R.J. Horizontal strain-rates and throw-rates across breached relay zones, central Italy: Implications for the preservation of throw deficits at points of normal fault linkage. \*Journal of Structural Geology\*, 31\(10\), pp.1145-1160, 2009.](#)
- Wallace, W.: *The laws which regulate the deposition of lead ore in veins: illustrated by an examination of the geological structure of the mining districts of Alston Moor*. E. Stanford, 1861.
- 520

- Walsh, J. J., and Watterson, J.: Analysis of the relationship between displacements and dimensions of faults. Journal of Structural Geology, 10, pp. 239-247, 1988.
- Walsh, J. J., and Watterson, J.: Distributions of cumulative displacement and seismic slip on a single normal fault surface. Journal of Structural Geology, 9, pp. 1039-1046, 1987.
- 525 Walsh, J. J., and Watterson, J.: Geometric and kinematic coherence and scale effects in normal fault systems, Geological Society, London, Special Publications, 56, 193-203, 1991.
- Walsh, J. J., Watterson, J., Childs, C., and Nicol, A.: Ductile strain effects in the analysis of seismic interpretations of normal fault systems, Geological Society, London, Special Publications, 99, pp. 27-40, 1996.
- Wells, D.L. and Coppersmith, K.J. New empirical relationships among magnitude, rupture length, rupture width, rupture area, and surface displacement. Bulletin of the seismological Society of America, 84(4), pp.974-1002, 1994.
- 530 Williams, G., and Vann, I.: The geometry of listric normal faults and deformation in their hangingwalls, Journal of Structural Geology, 9(7), pp.789-795, 1987.
- Withjack, M.O., Islam, Q.T., and La Pointe, P.R.: Normal faults and their hanging-wall deformation: an experimental study, AAPG Bulletin, 79(1), pp.1-17, 1995.
- 535 Withjack, M.O., and Schlische, R.W.: Geometric and experimental models of extensional fault-bend folds. Geological Society, London, Special Publications, 253(1), pp.285-305, 2006.
- Worthington, R.P., and Walsh, J.J.: Timing, growth and structure of a reactivated basin-bounding fault, Geological Society, London, Special Publications, 439(1), pp.511-531, 2017.
- Xiao, H.B., and Suppe, J.: Role of compaction in listric shape of growth normal faults, AAPG Bull., 73(6), 777-786, 1989.
- 540 Xiao, H., and Suppe, J.: Origin of Rollover, AAPG bulletin, 76(4), pp.509-529, 1992.
- Xiaoli, Z., Guangyu, H., Senqing, H., Zewei, Y., Hui, W., and Lu, L.: Improved Geometric Model of Extensional Fault-bend Folding, Acta Geologica Sinica-English Edition, 89(6), pp.1847-1857, 2015.

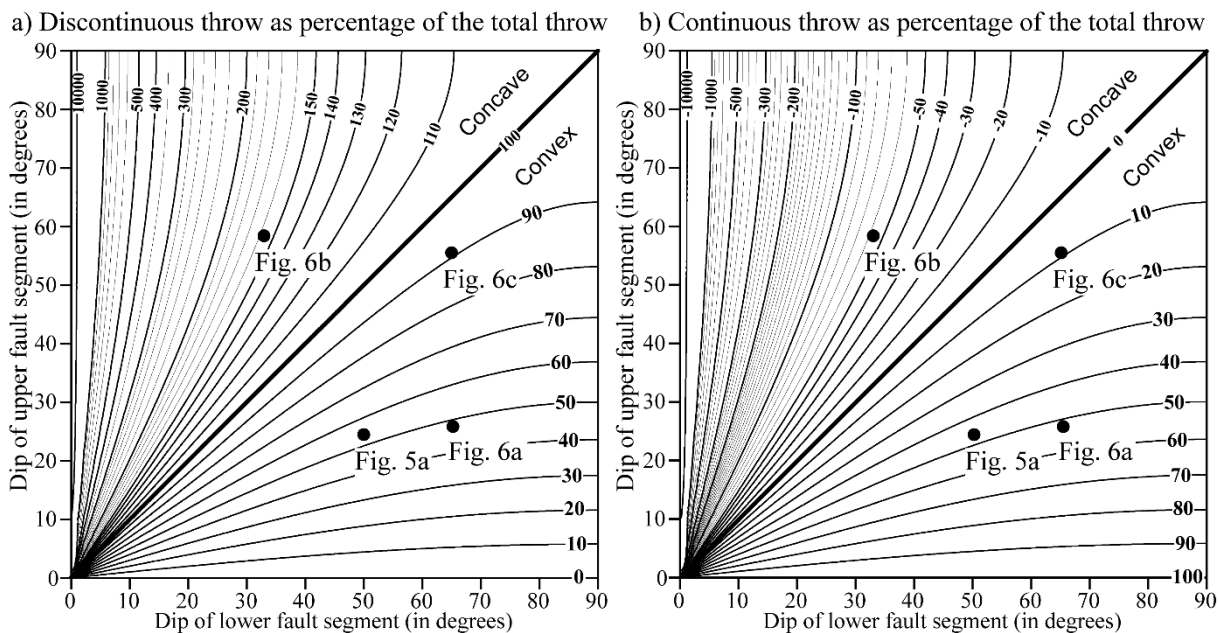


545

**Figure 1: Cartoons illustrating concave and convex fault bends and the associated hangingwall deformation in extensional and compressional tectonic settings.**



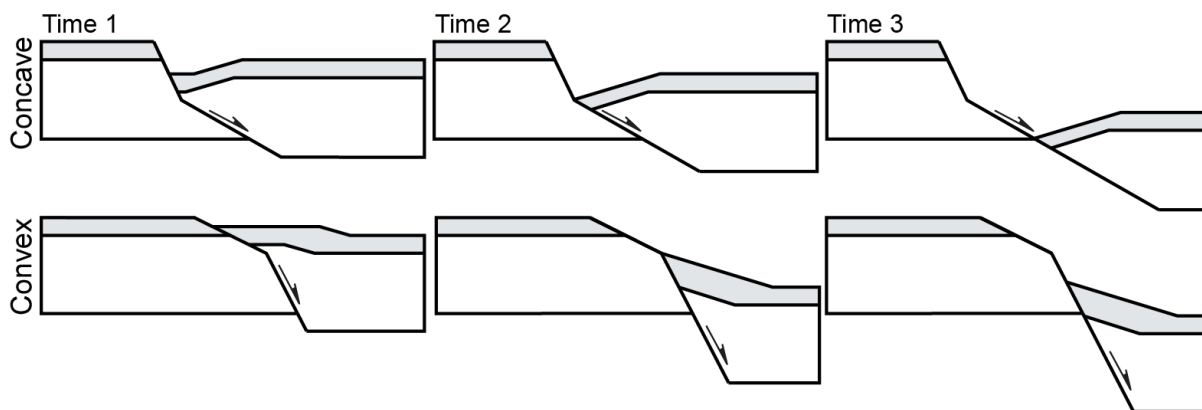
**550 Figure 2: (a) Schematic diagram of a fault that comprises three fault segments forming two sharp fault bends, a convex (bottom) and a concave (top). The total throw ( $T_t$ ) is partitioned into the discontinuous throw ( $T_d$ ) and the continuous throw ( $T_c$ ); the later comprises the antithetic continuous throw ( $AntC$ ) and the synthetic continuous throw ( $SynC$ ). (b) Throw-displacement profiles along the non-planar fault in (a) showing the complementary variations of the discontinuous and continuous throws given that the total throw and the displacement have a constant gradient that is not affected by the fault bends.**



555

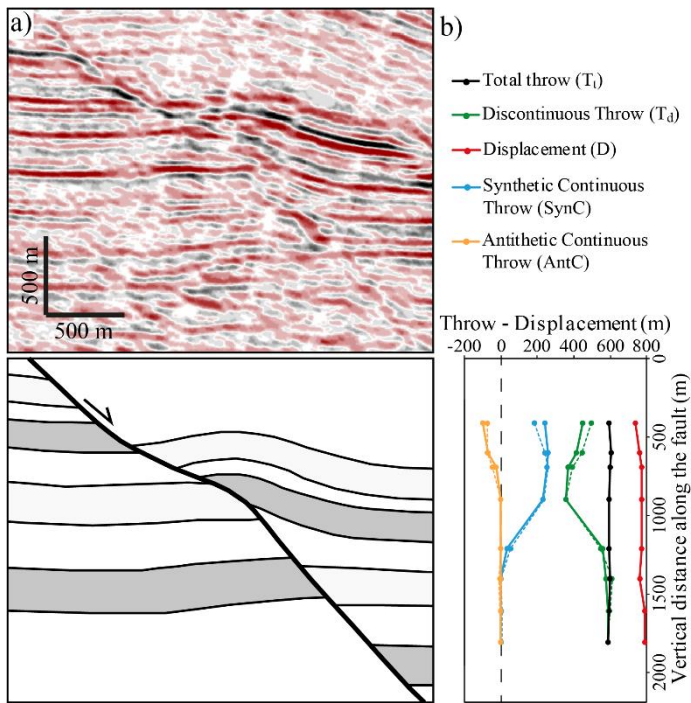
**Figure 3:** Graphs showing the modelled relationship between (a) the discontinuous ( $T_d$ ) and (b) the continuous ( $T_c$ ) throw, as a proportion of the total throw ( $T_t$ ), and the dips of the lower and upper fault segments of a sharp fault bend that comprises only two fault segments (i.e. Fig. 1). The geometries of the lower convex bends along the faults at Figs 5a and 6a, the upper concave bend along the fault at Fig. 6b and the convex fault bend at Fig. 6c are also plotted.

560

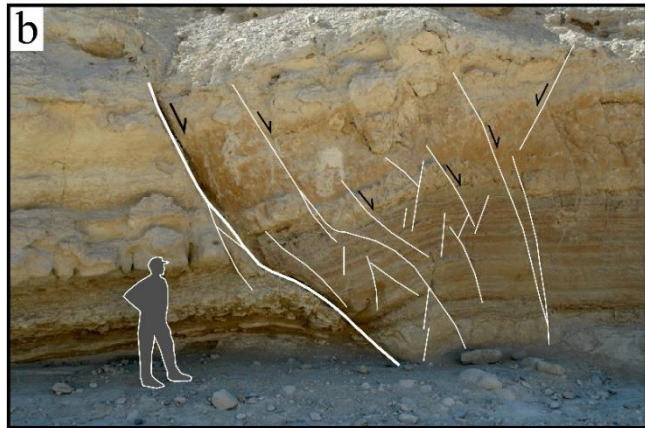
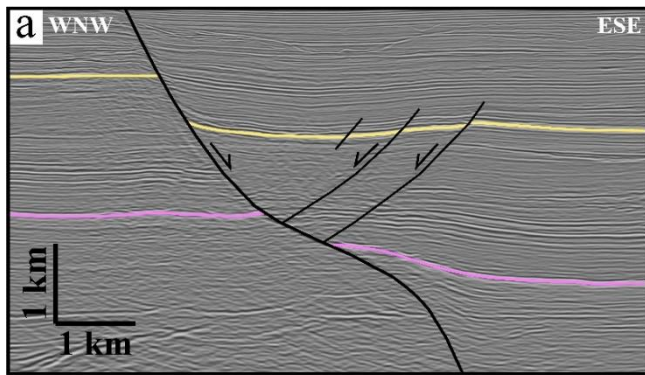


565

**Figure 4:** Block diagrams illustrating the evolution of the hangingwall deformation associated with a concave (top) and a convex (bottom) fault bend with increasing displacement at times 1 to 3. As soon as the hangingwall fault cutoff reaches the bend and begins to move along the lower fault segment (from time 2 to time 3), the absolute amount of continuous deformation doesn't increase anymore resulting in a progressive decrease of its proportion to the total throw.



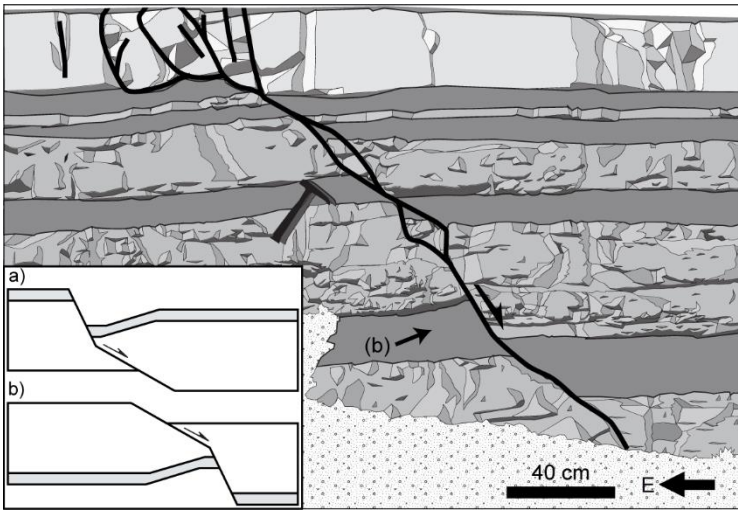
570 **Figure 5: (a) Uninterpreted and interpreted seismic profile of a non-planar fault and associated hangingwall deformation in the northwestern Porcupine Basin, offshore west Ireland. (b) Throw-displacement profiles along the fault in (a) showing the complementary variations of the discontinuous and continuous throws and the unaffected distribution of the total throw and the displacement by the fault bends. The modelled discontinuous and continuous throws are also plotted with dashed lines.**



575

Figure 6: (a) Interpreted seismic section of a non-planar fault and associated hangingwall deformation in the Taranaki Basin, offshore west of North Island, New Zealand. Deformation arises from movement on a fault bend produced by twisting and segmentation of an upward propagating fault (modified after Giba et al. 2012). (b) Outcrop example of a rollover anticline associated with a fault surface which has a sigmoidal shape from Wadi Matulla, Sinai, Egypt (modified after Fossen, 2016). (c) Outcrop example of a fault with 0.5 m throw contained within the Liassic limestone-shale sequence of Kilve, Somerset, UK, showing normal drag arising from a convex upward bend (and fault steepening). See text for more details.

580



585 **Figure 7: Outcrop sketch of a small normal fault from the Mesozoic South-Eastern Basin of France (after Roche et al. 2012). Pronounced reverse drag in the footwall of the fault occurs below the upward shallowing of the fault surface to display the geometry illustrated in the inset (b). Inset (a) is copied from Fig. 1 and (b) is (a) rotated through 180 degrees.**